Bulletin of the Seismological Society of America, Vol. 71, No. 5, pp. 1511–1530, October 1981

P_n VELOCITY ANISOTROPY IN SOUTHERN CALIFORNIA

BY UTE VETTER* AND JEAN-BERNARD MINSTER†

ABSTRACT

We analyze P_n propagation as a function of azimuth across a 28-station, 150-km aperture subarray of the SCARLET network centered near the central Transverse Ranges, California. We selected signals from 81 earthquakes and explosions with epicentral distances ranging from 150 to 400 km, covering all azimuths except a 40° gap from the southwest and a lesser gap from the northeast direction. For each source the apparent velocity of P_n was determined using a one-norm measure of misfit. The apparent P_n velocity does not show any systematic variation with epicentral distance but exhibits a strong azimuthal dependence. Our preferred interpretation calls for a slightly dipping (2° to N40W) planar moho, with 3 to 4 per cent anisotropy of subcrustal material. Transverse isotropy with a nearly horizontal symmetry axis is sufficient to explain the data; the direction of sagittal symmetry is N50W. The isotropic velocity of P_n is 7.8 km/sec. In contrast, a higher (8.1 km/sec) P_n velocity is found in the Mojave block, with no indication of anisotropy. These observations are consistent with a subcrustal model of the Pacific-North America plate boundary where ductile flow is characterized by simple shear in a vertical plane with strike parallel to the direction of relative plate motion.

INTRODUCTION

There is abundant evidence that the upper mantle in large portions of western North America is characterized by low P_n velocities (e.g., Herrin and Taggart, 1962; Pakiser and Steinhart, 1964; Herrin, 1969) and high attenuation (e.g., Solomon and Toksöz, 1970; Marshall *et al.*, 1979). Using arrivals from events to the north, east, and south, Kind (1972) further found an azimuthal variation of apparent P_n velocity in central California. Evidence for anisotropic propagation in the western United States was collected and analyzed recently by Bamford *et al.* (1979). They concluded that a small but significant amount of anisotropy (~3 per cent) can be documented, with a fast direction N70E to N80E, generally consistent with the offshore results of Raitt *et al.* (1969) for the Pacific upper mantle. However, the data set available to Bamford *et al.* (1979) consisted mainly of isolated profiles, each sampling the upper mantle in a different geographical location. Collating these data into a self-consistent set thus required a detailed time-term analysis such as the MOZAIC method developed by Bamford (1976).

In this paper, we focus on a very localized area, 150 km in aperture, and compare measurements of apparent P_n velocity in the same location, for a large number of directions with good azimuthal distribution. The dense SCARLET (Southern California Array for Research on Local Earthquakes and Teleseisms) short-period seismic network, monitored through the CEDAR (Caltech Earthquake Detection and Recording system) digital recording system, is particularly well suited for this purpose, thanks to a favorable distribution of natural and artificial seismic sources with azimuth and distance.

We find strong azimuthal dependence of P_n velocity in a 150-km-size region centered near the central Transverse Ranges. The most straightforward interpre-

* Present address: Seismological Laboratory, MacKay School of Mines, University of Nevada, Reno, Nevada 89557.
† Present address: Systems, Science and Software, P.O. Box 1620, La Jolla, California 92038.

tation of these observations calls for a gently dipping moho (2° to the NW) with 3 to 4 per cent anisotropy, the fast axis—also axis of sagittal symmetry—being subparallel to the San Andreas fault system. However, we could not detect any remarkable anisotropy in the Mojave Desert, to the northeast of the fault. Based on this comparison, we suggest that the observed anisotropy near the San Andreas fault system is diagnostic of subcrustal plate interaction along the Pacific-North America plate boundary, and discuss some of the possible interpretative models in the light of this hypothesis.

Observations and Data Reduction

The data set. Our prime consideration in selecting a subarray of SCARLET was that it should be well surrounded by seismic sources at P_n distances. Figure 1 depicts the outline of the subarray in relation to major tectonic features in southern California, and Figure 2 shows the 28 SCARLET stations and the 81 seismic sources retained for analysis. Except for a 40° gap from the southwest, and a paucity of sources from the east, this geometry affords good azimuthal coverage, and a fair spread of epicentral distances—from $\Delta = 150$ km to over 400 km from the centroid of the stations. The price paid for this selection is that the subarray samples the Mojave Desert to the north, the central and parts of the western Transverse Ranges, and the Los Angeles Basin to the south, so that it is underlain by a geologically and structurally variable crust, a potential source of complications. In a few isolated cases, we used additional stations located outside the outline on Figure 1 to help better constrain the P_n travel-time curve, particularly for directions where few sources were available.

Hypocentral information for the sources is given in Table 1. This list comprises mostly earthquakes with locations listed in the southern California Earthquake catalog (e.g., Hutton *et al.*, 1979) and a few Nevada Test Site (NTS) underground nuclear explosions listed in the U.S. Geological Survey (USGS) Preliminary Determination of Epicenters catalog.

Because our prime interest is in the apparent velocity of P_n, which is quite insensitive to epicentral errors, we did not relocate these events. Events prior to 1977 were timed from Develocorder films; for later events, we used archived CEDAR digital data, and analysis was performed interactively by computer. Only first P_n arrivals were timed, and we imposed a minimum magnitude threshold of $m_L > 3.5$—most events are actually significantly larger (see Table 1)—so as to avoid ambiguous, small amplitude arrivals. For a crustal thickness between 30 and 35 km, and source depth between 0 and 20 km, the crossover distance from P_g to P_n varies between 130 and 170 km. We only timed stations beyond the estimated crossover distance, and assigned a subjective quality factor to each pick: excellent, good, and fair, with nominal uncertainties of ±0.1, ±0.2, and ±0.5 sec, respectively. "Poor" picks, with a larger uncertainty, were not included in the analysis. Most events were well recorded by 15 to 20 stations, but we had to include some weaker events, with as few as 10 arrival times, in order to insure adequate coverage from some azimuths.

Data reduction. We determined a separate estimate of apparent P_n velocity for each event. Figure 3a shows the corresponding travel-time picks prior to any correction. Note that the apparent velocity derived from this graph is actually an azimuthal average since we do not deal with a linear profile but with an array. The azimuthal aperture of the subarrary shown on Figures 1 and 2 is 20° to 30° for the most distant sources and reaches up to 40° for the closest events. Apparent velocity

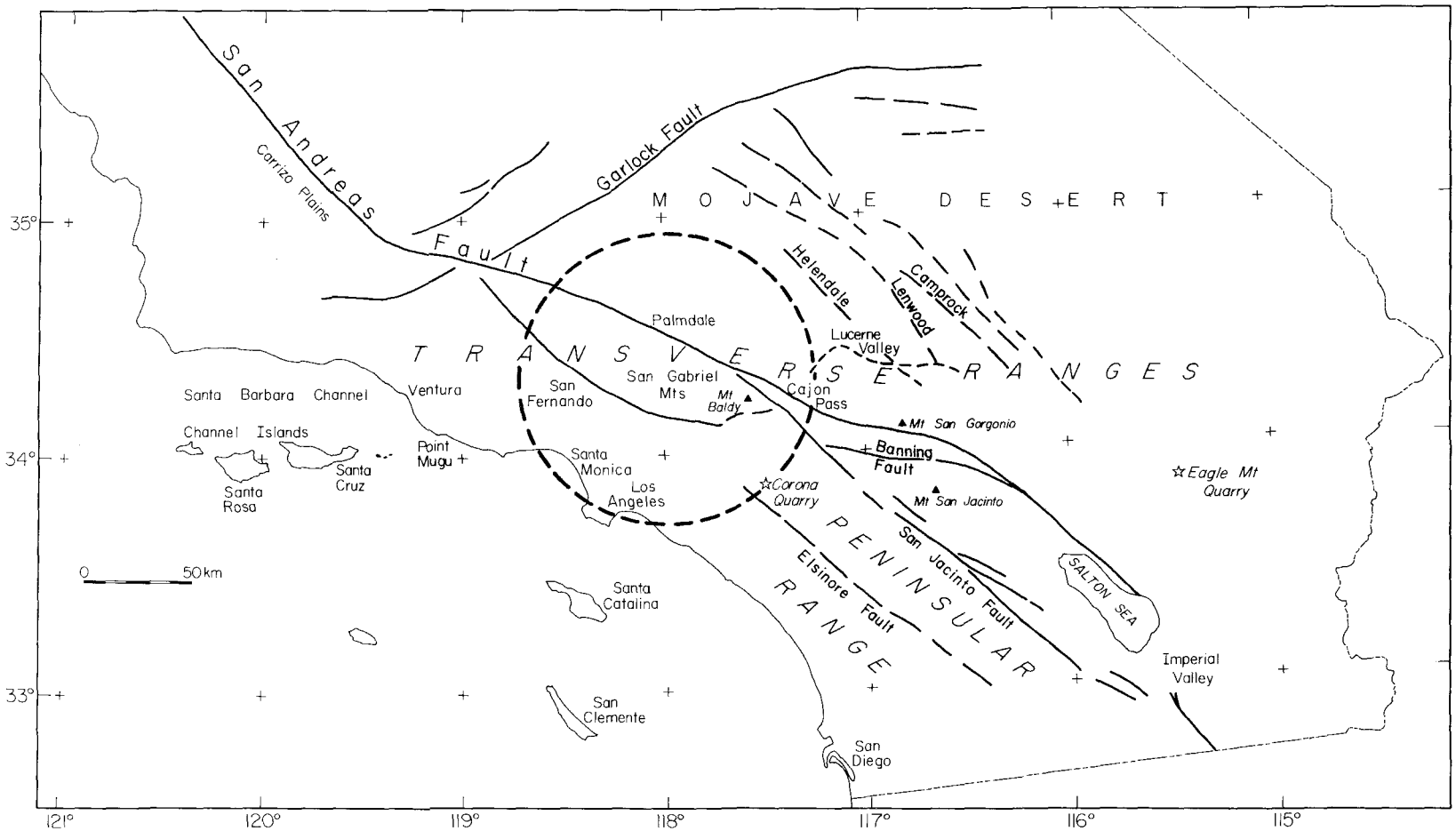

FIG. 1. Outline of the study area and of principal tectonic features in southern California.

estimates were obtained by first applying an elevation correction (surface velocity: 4.5 km/sec) and then fitting a cone with apex at $\Delta = 0$ to the observations.

In order to insure low sensitivity of the results to bad picks, particularly when few readings were available, we adopted a one-norm (L_1) measure of misfit (e.g., Claerbout, 1976), and minimized in each case

$$\epsilon_1 = \sum_{i=1}^{N} w_i^{-1} | t_0 + \Delta_i/V - t_i | \Big/ \sum_{i=1}^{N} w_i^{-1}. \tag{1}$$

Here the intercept time t_0 and apparent velocity V are adjusted to minimize ϵ_1

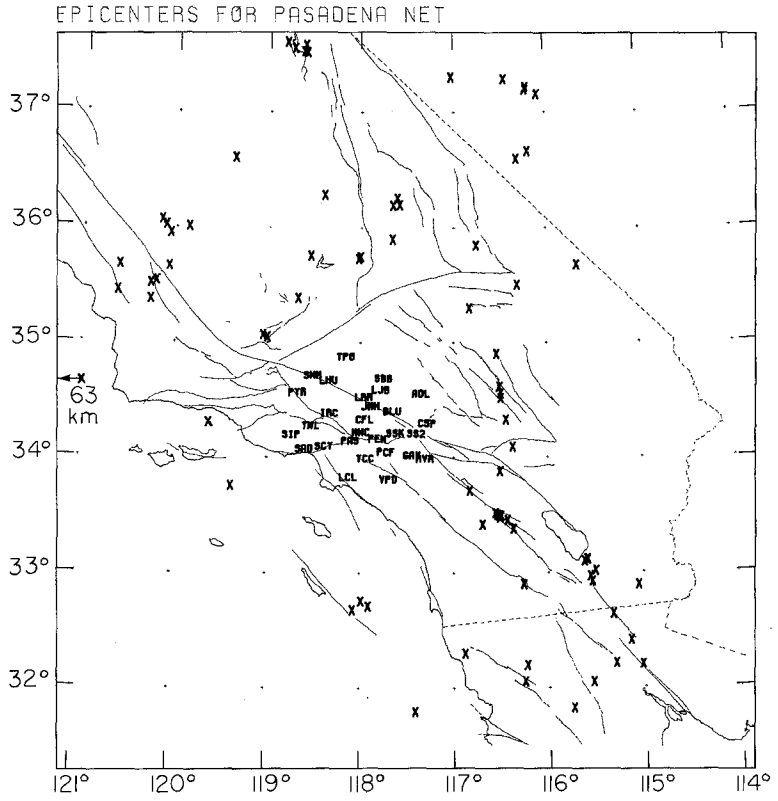

FIG. 2. SCARLET stations and epicenters used in this study.

knowing the N corrected times t_i and epicentral distances Δ_i. The weights w_i were chosen proportional to the nominal uncertainties described above.

Unfortunately, uncertainties in the adjusted parameters are not easily derived when L_1 adjustments are used (e.g., Parker and McNutt, 1980). In order to circumvent this difficulty, we first compared our results with classical least-squares (L_2 norm) estimates in a few test cases and found the two solutions to be in good agreement. We then assigned to each velocity estimate (L_1 norm) the formal uncertainty attached to the least-squares adjustment, assuming the error processes to be unbiased and Gaussian. We consider these uncertainties to be formal indicators of how well the velocity can be estimated from available data. We deliberately attempted to be conservative in the subjective estimates of timing errors and feel

TABLE 1

HYPOCENTRAL INFORMATION AND APPARENT P_n VELOCITY FOR SOURCES DEPICTED ON FIGURE 2

Year	Date	Time	Latitude	Longitude	Depth	Magnitude	Apparent P_n Velocity
1973	9 15	1 03 15.40	36 36.13	−119 22.52	8	4.4	8.42
1973	10 28	22 00 2.74	32 40.83	−118 04.64	8	4.5	7.53
1974	1 24	05 02 00.77	35 03.98	−119 02.94	6	4.3	7.94
1974	6 11	4 55 07.71	35 40.14	−115 40.10	8	3.8	7.12
1974	8 25	10 11 00.54	35 53.87	−117 39.42	1.4	3.8	7.97
1975	1 12	21 22 14.84	32 45.39	−117 59.29	15	4.8	7.60
1975	1 19	14 28 50.36	36 16.93	−118 23.83	5	3.8	7.80
1975	2 12	12 03 17.17	35 56.68	−120 03.96	16	3.9	8.04
1975	3 4	12 06 18.23	35 50.54	−116 45.03	8	3.6	7.55
1975	4 17	9 18 33.80	35 45.27	−118 32.53	10	4.0	8.23
1975	6 1	1 38 49.23	34 30.94	−116 29.73	4.5	5.2	8.07
1975	6 5	14 46 45.32	35 02.73	−119 00.03	9	4.1	8.07
1975	8 2	00 14 07.73	33 31.19	−116 33.48	13.4	4.7	7.84
1975	12 25	07 18 52.29	32 54.29	−116 15.63	36	4.0	7.41
1975	12 25	09 20 39.27	32 54.12	−116 15.49	3	3.7	7.67
1976	1 14	01 57 54.41	32 02.99	−115 32.21	13.8	4.1	7.52
1976	1 14	21 42 59.38	36 03.69	−120 09.75	7	4.7	8.26
1976	2 19	17 01 01.38	36 15.26	−117 36.39	3.9	4.0	7.68
1976	6 7	00 32 38.63	36 39.21	−116 11.57	12.3	4.1	7.68
1976	6 7	00 37 14.51	36 35.60	−116 18.92	17.8	4.1	7.73
1976	8 1	17 18 47.68	34 54.02	−116 32.34	5	3.5	8.16
1976	8 11	15 24 55.50	33 29.04	−116 30.78	15	4.3	7.73
1976	8 16	16 37 21.40	36 11.63	−117 39.31	8	3.7	7.97
1976	10 18	17 26 52.61	32 42.83	−117 54.61	15	4.2	7.52
1976	11 4	6 21 10.68	33 07.08	−115 35.73	5	4.1	7.66
1976	11 4	6 35 03.48	33 07.09	−115 35.41	4	4.1	7.79
1976	11 4	13 31 27.69	33 06.19	−115 37.31	3	4.2	7.69
1976	11 4	14 12 50.21	33 07.01	−115 35.73	5	4.4	7.77
1976	12 5	4 41 8.87	35 23.14	−118 40.50	0	3.8	8.06
1977	1 10	05 06 58.92	34 33.39	−116 29.57	8	3.8	7.71
1977	1 24	18 05 19.88	35 39.42	−120 04.49	5	3.7	8.19
1977	6 21	02 43 35.93	36 00.26	−119 51.97	4.8	3.8	8.28
1977	8 28	14 00 00.00	37 09.06	−116 05.16	0	4.8	7.83
1977	10 21	06 12 36.24	32 53.56	−115 03.29	5.9	4.3	7.54
1977	11 1	18 06 00.00	37 11.28	−116 12.78	0	4.7	7.60
1977	11 18	02 17 26.26	35 26.39	−120 37.18	4.9	3.6	8.07
1977	11 29	16 42 09.95	35 30.61	−120 15.85	4.8	3.9	7.96
1977	12 28	02 59 43.55	35 31.78	−120 12.42	4.9	3.6	8.32
1978	3 11	23 57 48.84	32 24.90	−115 08.73	6	4.8	7.60
1978	4 14	10 01 05.07	35 17.82	−116 49.74	7	3.6	8.05
1978	5 5	21 03 15.80	32 12.12	−115 18.21	6	5.2	7.66
1978	6 5	16 03 03.91	37 18.12	−116 41.88	12	4.4	7.80
1978	7 5	10 47 55.59	32 58.29	−116 30.32	0.4	3.8	7.74
1978	7 17	14 46 13.54	35 29.83	−116 18.61	5	4.0	7.07
1978	7 23	14 38 50.16	35 34.10	−120 15.98	5	3.5	8.08
1978	8 13	22 54 52.33	34 17.31	−119 37.58	5	5.1	7.92
1978	8 13	09 31 05.74	32 18.15	−116 52.85	19	4.1	7.50
1978	9 13	15 15 00.00	37 12.54	−116 12.66	0	4.6	7.63
1978	10 4	16 42 48.63	37 31.68	−118 37.89	9	5.8	7.93
1978	10 4	16 59 04.58	37 31.76	−118 38.06	12	4.4	8.10
1978	10 4	17 39 02.87	37 35.06	−118 37.04	10	5.3	8.11
1979	1 7	11 37 33.43	36 01.02	−120 06.89	5	3.8	8.10
1979	1 24	21 14 26.93	37 31.27	−118 36.22	5	4.4	7.66
1979	2 12	4 48 42.34	33 27.47	−116 26.05	4	4.0	7.71

TABLE 1—*Continued*

Year	Date	Time	Latitude	Longitude	Depth	Magnitude	Apparent P_n Velocity
1979	2 27	19 26 04.97	31 49.50	−115 44.88	5	4.4	7.69
1979	3 4	06 24 35.53	34 38.42	−121 41.61	5	3.9	8.06
1979	3 15	21 07 16.53	34 19.64	−116 26.69	3	5.2	7.89
1979	3 31	21 36 56.71	31 47.65	−117 24.61	5	4.7	7.56
1979	4 6	16 13 05.53	34 36.76	−116 30.66	5	3.7	7.65
1979	4 25	19 29 57.20	33 45.10	−119 22.30	7.2	3.5	7.81
1979	5 20	12 04 47.78	34 05.43	−116 22.20	1	3.7	7.50
1979	6 14	07 39 28.28	35 43.76	−118 01.40	5	4.6	7.91
1979	6 14	08 45 45.72	35 44.62	−118 00.34	5	3.7	7.87
1979	7 2	11 51 55.31	33 29.64	−116 30.08	5	3.7	8.41
1979	8 6	17 05 45.09	35 39.80	−120 36.56	5	5.9	8.24
1979	8 22	02 01 36.20	33 42.70	−116 49.70	18	4.1	7.79
1979	9 3	11 44 16.43	33 22.91	−116 22.23	5	3.9	8.30
1979	10 15	23 16 55.09	32 38.37	−115 19.68	6	6.6	7.71
1979	10 16	5 49 10.18	32 55.63	−115 32.38	10	5.1	7.74
1979	10 16	23 16 32.25	33 01.12	−115 30.23	15	4.9	7.56
1979	12 12	21 37 40.98	32 12.12	−116 13.73	5	4.0	7.64
1979	12 25	14 17 11.07	37 18.12	−117 01.87	6	4.1	7.73
1980	1 12	20 11 5.94	32 58.29	−115 33.35	5.3	4.1	7.50
1980	1 29	19 49 02.84	32 03.45	−116 15.07	5.4	4.4	7.78
1980	2 25	10 47 38.38	33 29.83	−116 30.81	14.23	5.5	7.99
1980	2 25	14 00 07.26	33 30.25	−116 32.25	5.2	3.7	7.58
1980	2 25	23 43 32.33	36 11.72	−117 35.02	5.4	3.9	7.66
1980	5 25	16 33 44.80	37 36.47	−118 49.27	3.2	6.0	8.02
1980	5 25	19 44 51.99	37 33.45	−118 44.55	6.5	6.3	8.10
1980	6 9	3 28 20.00	32 12.08	−115 01.69	?	6.7	7.68
1980	6 12	17 15 00.09	37 16.90	−116 27.23	0	6.6	7.77

that the induced error bars on the velocity are probably upper bounds. They range from ±0.03 km/sec (one-sigma error) in the most favorable cases to ±0.2 km/sec for the poorer events.

Apparent P_n velocities were found to range from 7.1 to 8.4 km/sec, with an overall average value of 7.83 km/sec. The distribution of these values with azimuth and epicentral distance Δ is illustrated on Figure 4. Because of the spread of Δ in our data set (Table 1), we looked for a variation of velocity with Δ, which would possibly indicate the presence of several travel-time branches (e.g., Hirn, 1977). As an example, the two rapid (~8.3 km/sec) arrivals seen on the figure for back azimuths between 50° and 60° might, in fact, be associated with the antiformal submoho structure proposed by Hadley and Kanamori (1977). However, the associated intercept times do not indicate an anomalous refractor depth, and these points have not been excluded from the analysis. Otherwise, no systematic correlation between velocity and distance can be detected within the scatter of observations on Figure 4, but there is an unmistakable azimuthal dependence. This variation is most clearly illustrated by the nonoverlapping 20° averages shown on the graph, with error bars estimated using Gaussian statistics. A 40° azimuthal gap remains from the southwest where no data could be collected. Note also that data from the northeast stem from very few weak events, and yield inconsistent velocity estimates, thus casting a doubt as to the proper identification of P_n. We chose not to use these data. The remaining 20° averages are used below instead of individual data for purposes of interpretation.

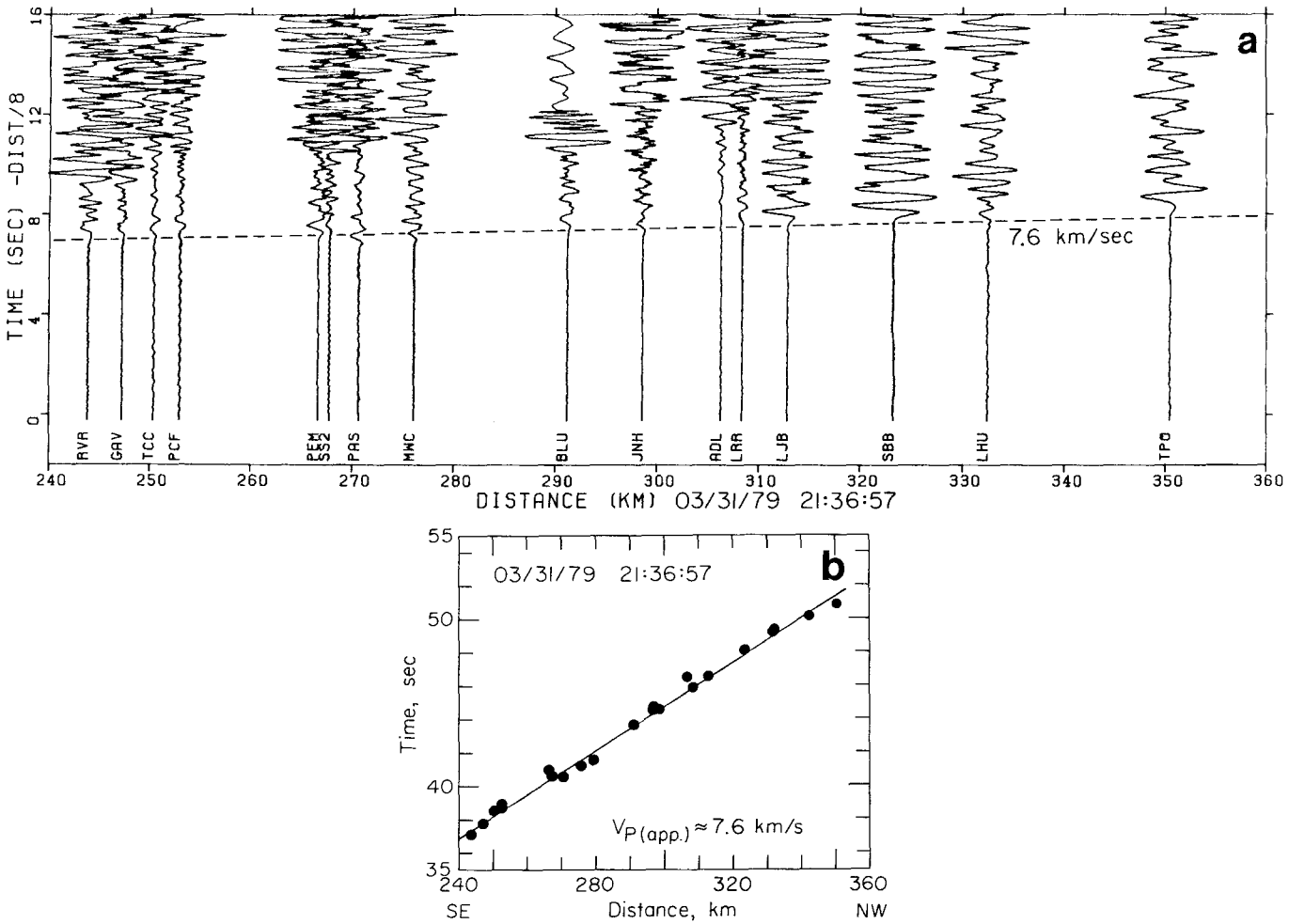

FIG. 3. (a) Typical seismic section across the subnetwork showing P_n arrivals with reduction velocity 8 km/sec. (b) Travel-time curve for event shown on (a) illustrating intrinsic scatter in the data.

MODELS

Lateral variations. Because of the rapid lateral changes in surface geology across the subarray (Figure 1), structural variations represent an obvious possible explanation of our data. The apparent P_n velocities determined in the previous section are displayed on Figure 5 on a polar diagram, with their error bars. Also shown is the best-fitting ellipse in a least-squares sense. (Note that the center of the polar diagram corresponds to 6.5 km/sec, and not zero, so that the curve drawn is *parallel* to an ellipse, and not an ellipse. Such distortion also holds for the following figures). The major axis of the ellipse is in the direction N51°W and passes through the center of the diagram to a very good approximation, so that it represents an axis of quasi-symmetry for the diagram.

An elliptical distribution of apparent velocity V_a with azimuth ϕ is what is expected for a planar, slightly dipping moho. We have

$$V_a(\phi) \simeq \frac{V_c}{\sin[i_c - \sin^{-1}(\sin \alpha \cos \phi)]} \approx \frac{V_t}{1 + \alpha \cot i_c \cos \phi} \tag{2}$$

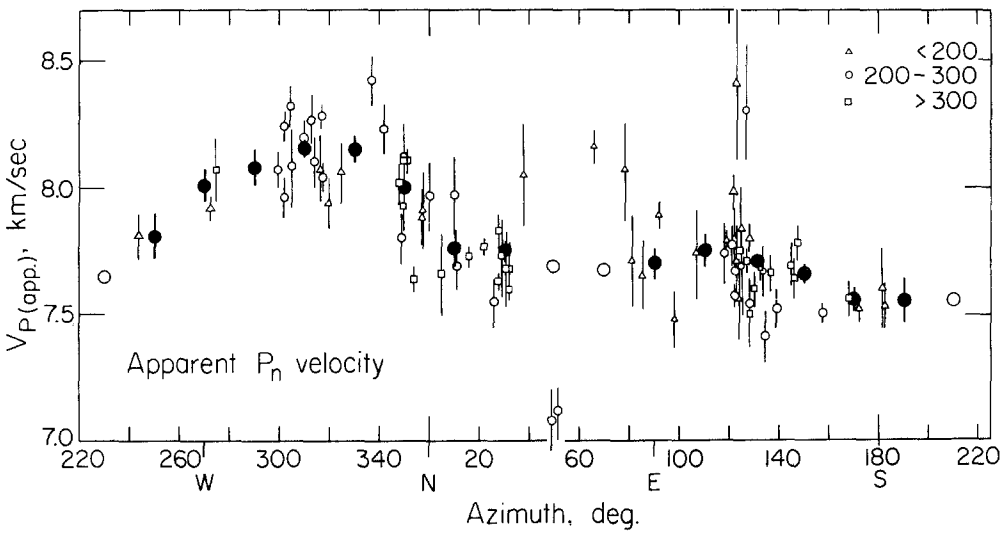

FIG. 4. Azimuthal variation of apparent P_n velocity across subnetwork. Symbols indicate different epicentral distance ranges. Full circles are nonoverlapping 20° means over azimuth. Open circles are interpolated and are not used in analysis.

where V_c is the crustal velocity, V_t the true moho velocity, $i_c = \sin^{-1}(V_c/V_t)$ is the critical angle, and the azimuth ϕ is measured from the dip direction.

Using the velocity estimates along the major axis and treating them as reversed profile estimates, with a mean crustal velocity of 6.2 km/sec (e.g., Hadley and Kanamori, 1977), we find a "true" moho velocity of 7.94 km/sec and a dip of about 2° to the northwest. For comparison, Hadley (1978) found a P_n velocity of 7.95 km/sec in the same region along a comparable direction, and concluded that moho dips 2° to 3° to the west beneath the eastern Transverse Ranges and southeastern Mojave.

However, the ellipse representing equation (2) has an eccentricity of 0.03, much smaller than the value of 0.3 for the best-fitting ellipse. We are thus led to introduce a more sophisticated model with moho curvature (e.g., Backus, 1965).

One alternative is to consider a synclinal moho topography, with an axis plunging slightly to the northwest. With a true moho velocity of 7.94 km/sec, the flanks of

this syncline would have slopes of about 3°. Because "reversed" profiles sample strongly overlapping sections of the moho with our 150-km aperture array, this is a lower bound estimate of moho slope. It corresponds to a 5-km decrease in crustal thickness per 100 km away from the syncline axis. In particular, this requires significant crustal thinning to the northeast, in the Mojave Desert, which is not supported by crustal studies (e.g., Hadley, 1978). An anticline with southwest-northeast axis, and a slight asymmetry—a steeper slope on the northwest flank—could also yield a similar pattern. "True" moho velocity would then be 7.65 km/sec, an uncomfortably low value. In addition, this model would predict an upward curvature of travel-time curves from the northwest or the southeast, a feature which we could not find in the data. Combination of these models could also be invoked, yielding a saddle-shaped moho, but these more complicated models unavoidably require a much greater degree of coincidence between structure and array geometry, which makes them somewhat less palatable.

Yet classes of models might be introduced, whereby variations in crustal thickness are replaced by lateral changes in crustal velocity or lateral variations in upper mantle velocity. While such variations undoubtedly exist in southern California, the remarkable degree of regularity and symmetry of Figure 5 makes such explanations rather unlikely to be correct, since they would rely once again on a precise coincidence of the inhomogeneity pattern with the array geometry.

Anisotropy. A general, yet simple class of models which can explain a regular azimuthal variation of P_n velocity involves a weak anisotropy of mantle material. In that case, the azimuthal dependence of the refractor velocity is of the form (Backus, 1965)

$$V_p^2(\phi) = C_p^2 + D_1 + D_2 \sin 2\phi + D_3 \cos 2\phi + D_4 \sin 4\phi + D_5 \cos 4\phi. \quad (3)$$

Here C_p is the isotropic wave speed and D_i, $i = 1, \ldots, 5$ are combinations of the elastic constants. Crosson and Christensen (1969) have specialized Backus's results to the case of transverse isotropy with arbitrary tilt of the symmetry axis, and showed that velocity data collected near the Mendocino and Molokai fracture zones can be explained under this assumption with a nearly horizontal axis. Transverse isotropy implies that a direction of sagittal symmetry should be present in the observations, and in that case equation (3) is actually of the form

$$V_p^2(\phi) = C_p^2 + D_1^* + D_3^* \cos 2(\phi - \beta) + D_5^* \cos 4(\phi - \beta) \quad (4)$$

where β is the azimuth of sagittal symmetry. A detailed discussion of the use of these relations is provided by Crampin and Bamford (1977). We first note that they both preserve the origin as center of symmetry, which is not the case on Figure 5. In fact, direct fitting of the 20° means by use of equation (3) yields an unacceptably poor solution. Thus, we first removed the shift in center of symmetry of the figure by correcting the data for a simple moho dip. We used a 2° dip in the N51°W direction, with $V_c = 6.2$ km/sec and $V_t = 7.94$ km/sec. The reduced estimates were then fitted by equation (3) using a least-squares criterion

$$V_p^2(\phi) = 60.70 - 2.13 \sin 2\phi - 0.64 \cos 2\phi - 0.01 \sin 4\phi + 0.01 \cos 4\phi. \quad (5)$$

Under the assumption that there exists a direction of sagittal symmetry, we can

then estimate its azimuth β by using $\beta = \frac{1}{2} \tan^{-1} (D_2/D_3)$ (e.g., Crampin and Bamford, 1977). This yields the two solutions N37°E and N53°W. We also have $\beta = \frac{1}{4} \tan^{-1} (D_4/D_5)$ which yields four solutions N34°E, N79°E, and N11°W, N56°W. Although the agreement favoring N53°W and N37°E as symmetry axes is encouraging, this argument is weak because D_4 and D_5 are small and poorly determined by the data. More specifically, the lack of observations from the northeast and southwest places serious doubts on the reliability of D_4 and D_5. A data fit as good as that provided by equation (5) can be achieved using equation (4) in the form

$$V_p^2(\phi) = 60.70 - 2.19 \cos 2(\phi - 37.1) - 0.003 \cos 4(\phi - 37.1). \quad (6)$$

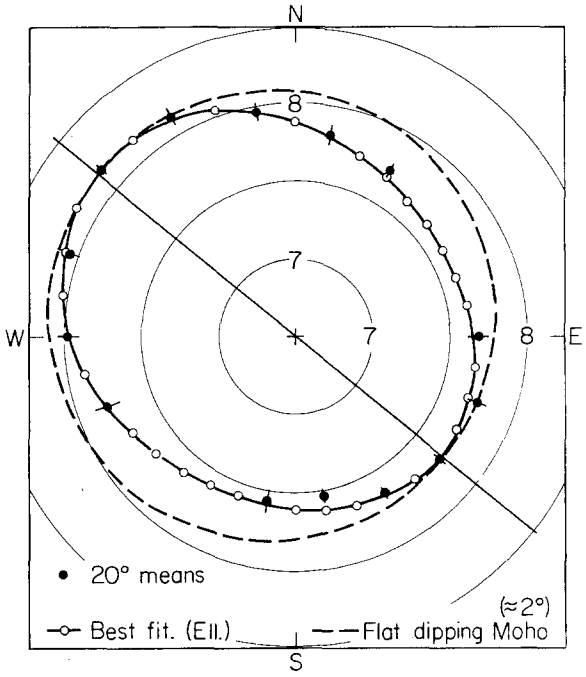

FIG. 5. Polar diagram representation of 20° means and associated statistical uncertainties. Solid line represents least-squares ellipse, and dashed line is ellipse calculated for planar moho dipping 2° in N51W direction [equation (2) of text].

If D_1 is assumed to be small—a common result (e.g., Backus, 1965; Crosson and Christensen, 1969)—then $C_p \sim 7.79$ km/sec, in good agreement with the upper mantle velocity of 7.8 km/sec estimated by Hadley (1978). Figure 6 illustrates the fits to the dip-corrected 20° means provided by equation (6). The curves corresponding to equations (5) and (6) would not be visibly different. We can achieve a slight improvement in fit by an iterative process and use the estimate 7.8 km/sec to remove moho dip. In that case, equation (6) is replaced by

$$V_p^2(\phi) = 60.6 + 2.22 \cos 2(\phi + 60) + 0.001 \cos 4(\phi + 60) \quad (7)$$

and the largest residual is only 0.08 km/sec.

Rather than estimating separately dip and anisotropic properties of the moho, we

can estimate them simultaneously by using a fitting function of the form

$$V_p^2 \approx \frac{C_p^2 + D_1^* + D_3^* \cos 2(\phi - \beta) + D_5^* \cos 4(\phi - \beta)}{(\cos \alpha' - \text{cotan } i_c \sin \alpha')^2} \tag{8}$$

with

$$\alpha' = \sin^{-1}[\sin \alpha \cos(\phi - \psi)] \tag{9}$$

where β measures the azimuth of sagittal symmetry, α is the dip angle, and ψ is the dip direction. With a mean crustal velocity of 6.2 km/sec and a moho velocity of 7.8

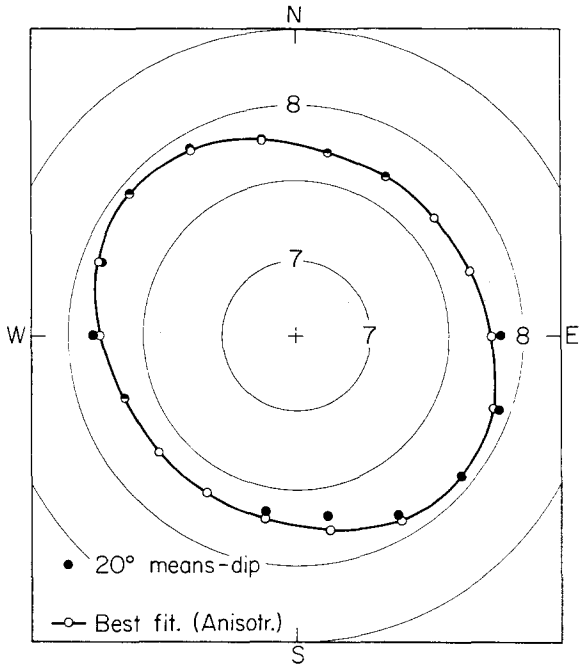

FIG. 6. Fit to 20° means, corrected for planar moho dip, and assuming transverse isotropy with horizontal symmetry axis [equation (6) of text].

km/sec, we get an isotropic velocity of 7.79 km/sec, $D_3^* = 2.2$, $D_5^* = 0.01$, $\beta = -49.5°$, $\alpha = 2.1°$, and $\psi = -40°$. The fit is shown on Figure 7 and is excellent. Variations of the assumed mean crustal velocity in the range 6.2 to 6.8 km/sec lead to small changes in the solution where ψ varies between $-42°$ and $-38°$. As expected, the constant D_5^* is the most poorly determined parameter, but it remains in all cases much smaller than D_3^*. This is in agreement with the conclusion of Crampin and Bamford (1977) who find a cos 4ϕ term six times smaller than the cos 2ϕ term for olivine crystals. These authors point out that D_5^* could provide a potential discriminant between various models of anisotropy, but that its determination is usually quite uncertain due to its sensitivity to measurement errors.

Based on this calculation, our favored interpretation of the 20° means involves a slightly dipping (~2°) moho, in the direction ~N40°W, with an isotropic velocity of 7.8 km/sec and a 3 to 4 per cent anisotropic—transversely isotropic—upper mantle material, with a fast axis in the ~N50°W direction. The sequence of calculations described above suggests that these azimuths are uncertain by about 10°, although

a statistical estimate of uncertainty (e.g., Crosson, 1972) would require a larger data set.

Station corrections. Aside from elevation corrections, we did not apply station corrections, which might be associated with local subreceiver structure. Residuals to the L_1 fits from individual events show some stations to be generally late, and others generally early; a few display an azimuthally varying delay. The question at hand is whether station corrections could significantly alter our results. In order to test this possibility, we applied station corrections using the following iterative procedure.

Individual station delays were estimated using 16 well-timed events with good azimuthal distribution. Velocities were then estimated anew, and the station delays again determined. This bootstrapping procedure was iterated four times. The first three iterates are shown on Figure 8, with the corresponding least-squares ellipses.

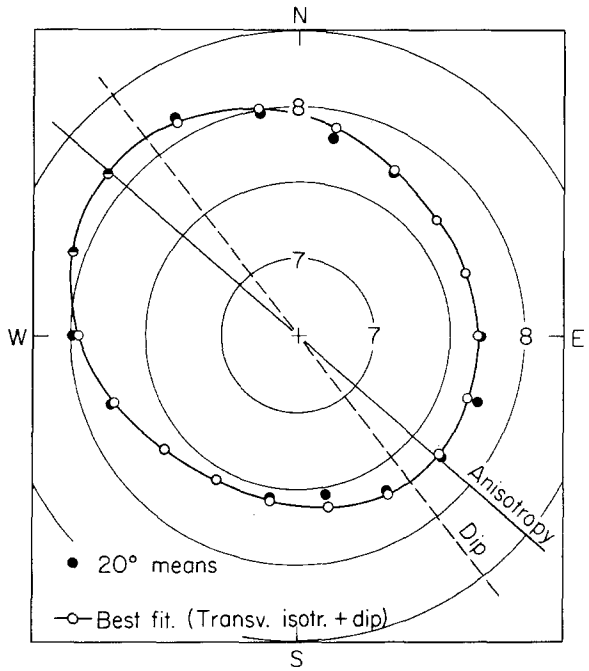

FIG. 7. Simultaneous fit to uncorrected 20° means assuming plane-dipping moho and transverse isotropy with horizontal symmetry axis [equation (8) of text].

(The algorithm converged rapidly and the fourth iterate is undistinguishable from the third.) The method yields a slightly steeper dip angle, but no change in dip direction. In view of the uncertainty in the velocity estimates, this correction appears to be a minor one and we feel justified in attempting to interpret the uncorrected results below.

INTERPRETATION AND DISCUSSION

Comparison with earlier measurements. Recent crust and upper mantle studies in the same area by Kanamori and Hadley (1975), Hadley and Kanamori (1977), and Hadley (1978) were based on reversed or nearly reversed profiles using local earthquakes and explosions. The results are summarized on Figure 9. East-west profiles tend to exhibit greater P_n velocities than north-south profiles, in accordance with our results. Note the remarkable agreement of the value they obtained in our study area, 7.95 km/sec, with our estimate of 7.94 km/sec in the same azimuth. The

east-west structural profile depicted in Figure 9b in our study area shows little change in crustal thickness, with a 2° to 3° moho dip to the west; it does suggest variations in the mean crustal velocity over our subarray, but we have shown that our results are not very sensitive to this parameter. No north-south profile is given in our area of interest, but little north-south change in crustal thickness is detected further east (Hadley, 1978). The fast (8.3 km/sec) travel-time branches shown on Figure 9b are interpreted by the authors in terms of an antiformal structure trending east-northeast, and culminating about 40 km below the moho. We believe that this structure is not sampled by our data. All in all, the conclusions of Hadley and Kanamori are consistent with ours, and are generally more consistent with our interpretation in terms of moho anisotropy, as opposed to moho topography.

Anisotropy of P_n was suggested by Kind (1972) for central California data. Kind

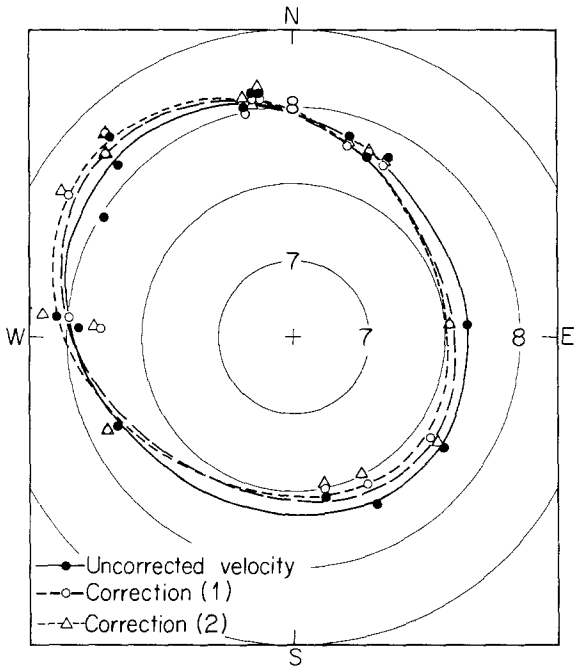

FIG. 8. Effect of iteratively determined station corrections using 16 well-timed events. Three iterations are shown with corresponding best-fitting ellipses. Subsequent iterations do not lead to further changes.

found higher velocities for arrivals parallel to the San Andreas than for events from the east. This would tend to agree with our results. In particular, this orientation of the fast axis is quite different from that found by Raitt *et al.* (1969) off the California coast where the high-velocity azimuth is subparallel to the spreading direction. Bamford *et al.* (1979) reinterpreted refraction profiles in the western United States using the MOZAIC time-term method developed by Bamford (1976). Only one of their profiles (Santa Monica-China Lake) crosses our study area. These authors find a 2 to 3 per cent anisotropy, with faster velocities in the N70° to 80°E direction, in fair agreement with offshore data. They explain it as a possible consequence of mesozoic lithospheric subduction. In particular, they support the opinion of Snyder *et al.* (1976) that late mesozoic and oligocene magmatic arcs extended parallel to the coast and were associated with back-arc spreading. Anisotropy would then be caused by crystal alignment in the tensional direction, which would more or less coincide with the offshore spreading direction.

The discrepancy between the results of Bamford *et al.* (1979) and the conclusions

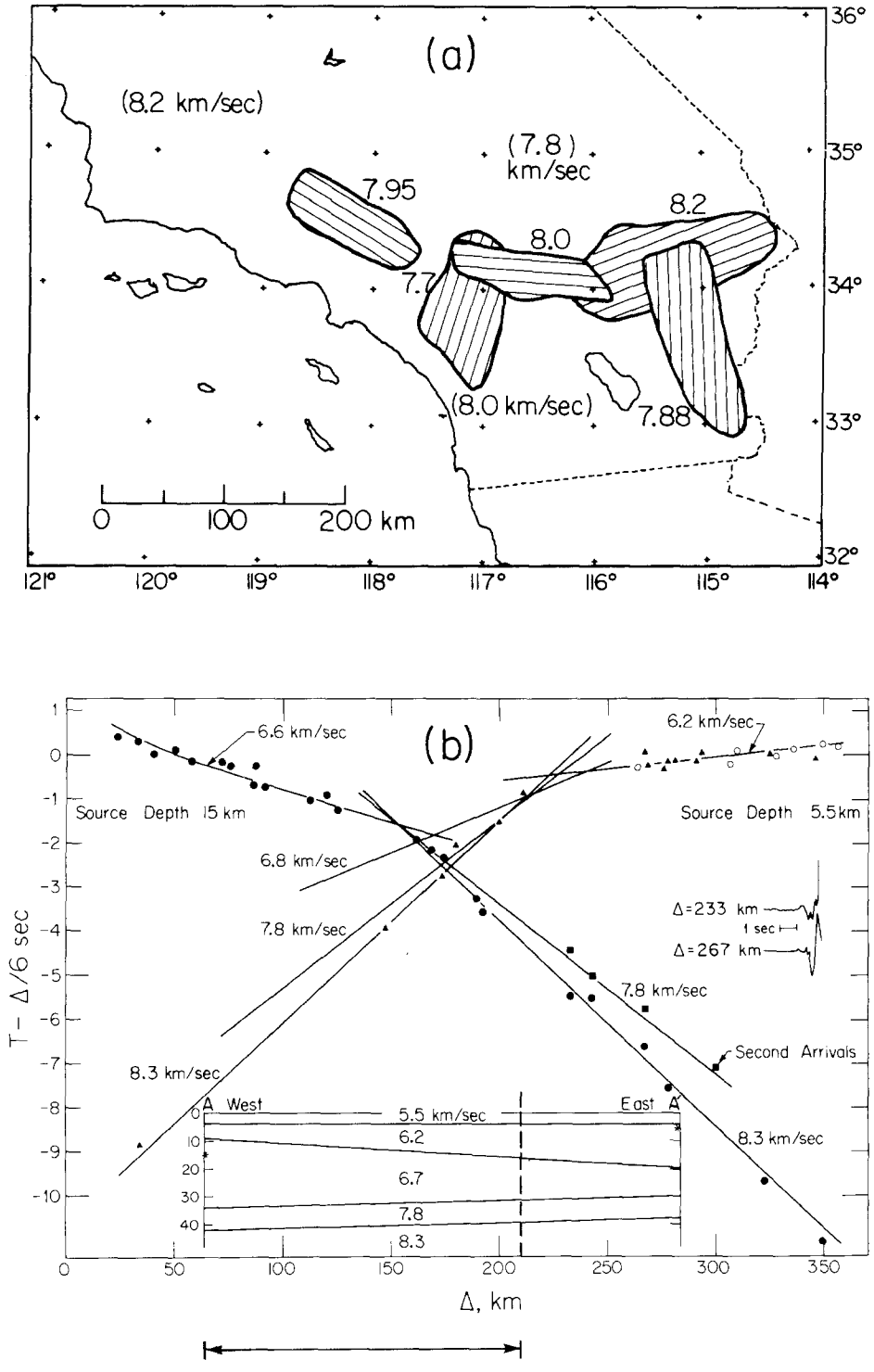

FIG. 9. (a) Outline of geographical areas covered by previous P_n studies, and dominant azimuth of profiles (after Hadley, 1978). (b) East-west profile and crustal model crossing study area (indicated by the *arrow*), showing travel-time curve and crustal model across the network of Figure 2 (after Hadley, 1978).

of the present study may stem from the vast differences in the regions sampled by the profiles. They collected data covering a large area in the western United States and reduced them under the implicit assumption of lateral structural coherence, whereas the present study focused exclusively on a small (150-km) region near the plate boundary. Additional studies similar to the present one in different areas are needed to address the question of lateral variations.

P_n velocity variations in the Mojave. A preliminary test of lateral variations can be attempted by considering another subarray of SCARLET located in the Mojave Desert (Figure 10). The geometry is less favorable, and the network not as compact. Only 13 events were analyzed (Table 2, Figure 10). Hadley and Kanamori (1977)

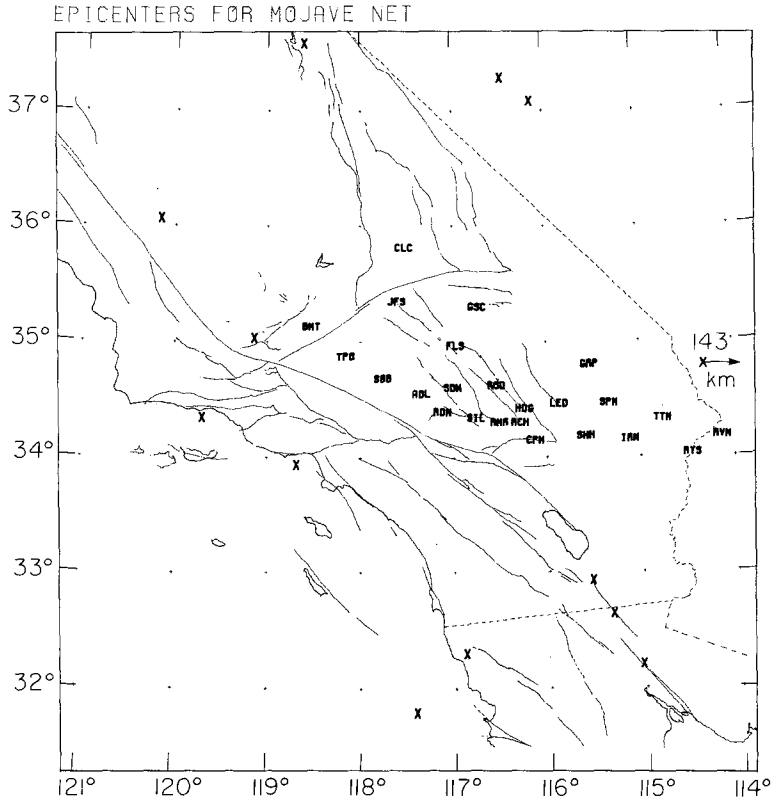

FIG. 10. Stations and sources used in study of Mojave block.

proposed a partial offset of the Pacific-North America plate boundary below the crust under the Mojave block. Instead of following the San Andreas fault, the plate boundary would lie beneath the active Helendale-Lenwood-Camprode fault trend, which cuts the Mojave in the NW-SE direction. Because the Mojave network shown in Figure 10 is so spread out we also attempted, whenever possible, to derive independent P_n velocity estimates from only the western or the eastern halves. Otherwise, the analysis was carried out following the same procedure as described above. The resulting P_n apparent velocities are listed in Table 2. (Because of the small number of events, we omitted the 20° averaging over azimuth.)

The results can be summarized as follows

1. For the whole Mojave network: P_n velocity of 8.05 km/sec, with a moho dip of 1.3° to the west (~N86W).
2. For the western Mojave: P_n velocity of 7.99 km/sec, with a moho dip of 1.5° to the west (N88W).
3. For the eastern Mojave: P_n velocity of 8.11 km/sec with a moho dip of 1.3° to the west (N74W).

TABLE 2

HYPOCENTRAL INFORMATION AND APPARENT P_n VELOCITY FOR SOURCES USED IN CONJUNCTION WITH THE MOJAVE NETWORK (FIGURE 10)

Year	Date	Time	Latitude	Longitude	Depth	Magnitude	Apparent P_n Velocity
1976	1 14	21 42 59.38	36 03.69	−120 09.75	7	4.7	8.05
							(E: 8.28)
1976	2 04	00 04 57.10	34 44.20	−112 27.80	8	4.7	7.98
							(E: 7.97)
							(W: 7.83)
1978	2 23	17 00 00.65	37 04.74	−116 02.27	5	5.4	7.92
							(E: 7.95)
							(W: 7.77)
1978	6 16	4 21 31.63	35 02.08	−119 08.23	1	4.3	8.09
							(E: 8.03)
1978	8 13	22 54 53.42	34 20.82	−119 41.76	12	5.1	8.27
							(E: 8.26)
1978	8 19	9 31 05.74	32 18.15	−116 52.85	19	4.1	8.03
1978	10 04	17 39 02.87	37 35.06	−118 37.04	10	5.3	8.00
							(E: 8.05)
							(W: 7.98)
1979	1 01	23 14 38.94	33 56.66	−118 40.88	11	5.0	8.19
							(E: 8.19)
							(W: 8.21)
1979	3 31	21 36 56.71	31 47.65	−117 24.61	5	4.7	7.96
							(W: 8.06)
1979	10 15	23 16 55.09	32 38.37	−115 19.68	5	6.6	7.76
							(W: 7.84)
1979	10 16	5 49 10.18	32 55.63	−115 32.38	10	5.1	7.96
							(E: 8.15)
							(W: 7.97)
1980	6 09	20 28 20.00	32 12.08	−115 01.69		6.7	8.15
							(E: 8.07)
							(W: 8.25)
1980	6 12	17 15 00.09	37 16.90	−116 27.23	0	6.6	7.97
							(W: 7.81)

In neither case did we find it necessary to invoke anisotropy to explain the data depicted on Figure 11. The fit is good for data from the west, south, and east, but apparent P_n velocities from the north are smaller than predicted, possibly due to nonplanar moho structure, although this hardly constitutes a convincing argument. Postulating a small amount of anisotropy does not improve the fit significantly.

Although this test is not a definitive one, due primarily to the paucity of data, it does appear that (1) the velocity of P_n is higher beneath the Mojave than beneath the central Transverse Ranges, and (2) anisotropy of submoho material is not as

pronounced, or may even be nonexistent away from the San Andreas fault to the northeast.

A tectonic interpretation. The San Andreas fault is the most prominent surface expression of the Pacific-North America plate boundary. However, as seen on Figure 1, the network which we used in this study lies astride a major tectonic complication, namely the "big bend" of the San Andreas fault. The depth extent of this geometrical complication certainly involves the seismogenic layer (15 to 20 km) and probably the entire crust. However, Hadley and Kanamori (1977) found an upper mantle velocity anomaly more or less coincident with the Transverse Ranges which is not offset by the fault. In their interpretation, the subcrustal plate boundary does not

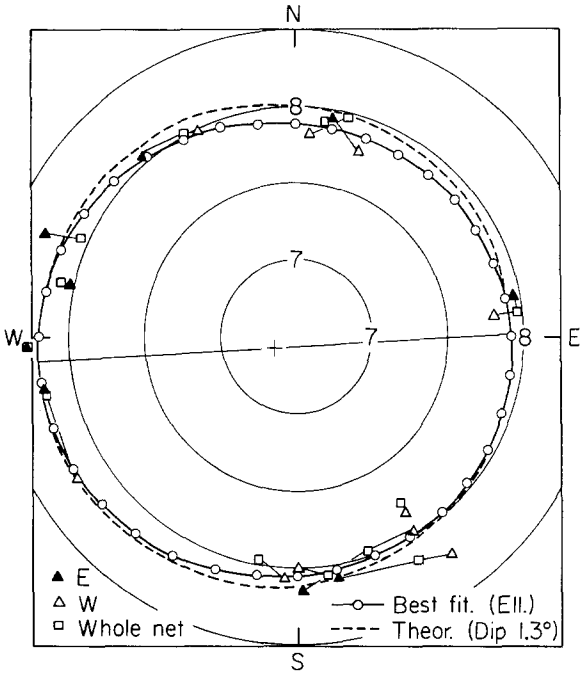

FIG. 11. Polar diagram representation and best-fitting ellipses to data for Mojave block. When possible, separate estimates for eastern and western Mojave are shown.

follow the big bend, but is rather aligned with the southern portion of the fault. Thus, the plate boundary at depth extends from the Salton trough to the south to a line crossing the central Mojave Desert. Because of this difference in geometry between the surface features and the plate boundary at depth, they require a decollement decoupling the superficial layer from the deepest part of the lithosphere.

In central California, the San Andreas fault is a simple strike-slip feature along which a good portion of the relative motion between the Pacific and North American plates takes place and there is little reason to think that the subcrustal plate boundary in central California does not coincide with the surface feature. We must therefore model a westward offset of almost 100 km of the plate boundary in the upper mantle between the central Mojave Desert and the San Andreas fault in central California.

The area sampled by our data set, as shown on Figure 1, lies in a symmetric position with respect to the Fort Tejon and Fort Cajon bends in the San Andreas fault, and thus can be expected to yield information about the subcrustal offset of the plate boundary. It is primarily characterized by low P_n velocities, and according

to our preferred model, by anisotropy with a fast direction subparallel to the general trend of the San Andreas fault, and therefore to the azimuth of relative plate motion. According to Christensen and Salisbury (1979), the 0.2- to 0.3-km/sec drop in velocity between the observed value of 7.8 km/sec and the more classical value of 8.1 km/sec found in the Mojave could be explained by an increase of temperature near moho depth of 200° to 300°K. Although it may be tempting to associate this possibility with the upper mantle velocity anomaly found below moho by Hadley and Kanamori (1977), such a temperature difference would mean a 20 to 40 per cent heat flow anomaly at the surface, which is not observed in that region (Lachenbruch and Sass, 1980). In addition, the upper mantle flow solution near the big bend proposed by Bird (1980) attempts to interpret the velocity anomaly of Hadley and Kanamori by a down-welling pattern associated with colder temperatures. An alternative model involving the addition of low-velocity components (e.g., pyroxene) and possible serpentinization would explain the low velocities while preserving anisotropy (e.g., Christensen and Crosson, 1968; Christensen and Salisbury, 1979).

The anisotropy pattern invoked in our model is a more diagnostic feature. Christensen and Crosson (1969) found that in many cases (1) the olivine *b* axes (low velocity) in ultramafic rocks tend to be concentrated normal to the schistosity or banding with the *a* and *c* axes forming girdles normal to the *b*-axis concentration or (2) the *a* axes are bundled, with the *b* and *c* axes arranged in girdles in the orthogonal plane. Either arrangement results in transverse isotropy for compressional waves. On the other hand, Raleigh (1968) found experimentally that *a* axes of olivine deformed at low-strain rate and temperature tend to align themselves parallel to the direction of shear by pencil glide. In the geometry shown on Figure 1, the region covered by this study lies close to the center of symmetry of the required offset of the subcrustal plate boundary. A reasonable flow regime in that region is likely to be locally dominated by simple shear (right lateral) in a vertical plane trending parallel to the direction of relative plate motion (~N40W) (Minster and Jordan, 1978). In that case, we expect the *b* axes to be statistically concentrated in the ~N50E direction, and, if pencil glide takes place, the *a* axes to be oriented in the N40W direction. These azimuths compare favorably with the symmetry directions (N50W, N40E) of our observations. Transverse isotropy of the kind proposed by Crosson and Christensen (1969), with a nearly horizontal axis of symmetry, is consistent with this model and adequately explains the observations. The moderate amount of anistropy (3 to 4 per cent) which we found is easily explained by invoking a less-than-perfect crystalline orientation (e.g., Crosson, 1972) or a mixture of isotropic and anisotropic materials (e.g., Crampin and Bamford, 1977).

Early measurements of anisotropy were practically confined to the Pacific Ocean, and were recently reviewed by Fuchs (1977). In these cases, the high-velocity direction coincides well with the spreading direction. A classical interpretation involves alignment of the *a* axes parallel to the spreading direction by pencil glide during the creation of new lithosphere (Raleigh, 1968; Peselnick *et al.*, 1974). Bamford (1976) found a fairly large degree of anisotropy (7 to 8 per cent) in southern Germany and noted that the fast axis (N15 to 20°E) may be correlated with the direction of absolute motion of the European plate. Again, he invoked alignment of the *a* axes of olivine by pencil glide. In the present study, distinction between a model invoking alignment of *a* axes and one invoking alignment of the *b* axes would require a measurement of the vertical *P* velocity below moho. This is at best a difficult task, and the model must remain ambiguous in that respect.

Conclusions

The azimuthal dependence of apparent P_n velocity in a 150 km diameter region of southern California centered near the central Transverse Ranges is most easily explained by a slight dip (~2°) of the moho in the direction N40W coupled with about 2 to 3 per cent anisotropy. Transverse isotropy, with a nearly horizontal symmetry axis is sufficient to explain the observations. The symmetry axis may be associated either with the alignment of b axes of olivine in the N40E direction or with the alignment of a axes in the N50W direction, which are more or less orthogonal and parallel to the direction of relative plate motion, respectively. The data cannot resolve these two alternatives. The isotropic velocity of P_n is only 7.8 km/sec, which may be due to serpentinization and/or mixture with low-velocity components. For comparison, we found that P_n velocity is isotropic and is 8.1 km/sec in the Mojave block, although these conclusions are based on much fewer data.

These observations can be explained within the framework of a simple tectonic model of the subcrustal Pacific-North America plate boundary near the big bend of the San Andreas fault. Specifically, we propose that the westward offset of the San Andreas fault between the northern part of the Salton trough and central California is accommodated by a regime of simple shear—at least locally—beneath the crust. This model is very similar to the plate boundary model proposed by Lachenbruch and Sass (1980) whereby the narrow fault zone which characterizes the seismogenic layer gives way to a broad zone of simple shear deformation extending to the bottom of the lithosphere. The model requires a decollement or decoupling zone below the seismogenic layer, as proposed by Hadley and Kanamori (1977) beneath the San Gabriel Mountains. Further evidence for the existence of such a decollement is provided by Corbett and Johnson (1981) in their study of the Santa Barbara earthquake of 1978. In addition, the geodetic data collected by Savage *et al.* (1981) in the same region can be modeled by a horizontal southward-propagating dislocation beneath the Transverse Ranges. On the other hand, the high-velocity subcrustal structural trend discovered by Hadley and Kanamori (1977) in the same area does not show any evidence of right-lateral shearing, and thus the regime of simple shear which we propose may not extend to the base of the lithosphere.

Acknowledgments

We are grateful to D. L. Anderson and H. Kanamori for useful discussions. C. Johnson and P. German were very helpful in retrieving CEDAR data and provided the computer program to compute apparent velocities using the L_1 norm. W. L. Rodi provided helpful comments which led to improvements in the manuscript. Further comments from S. Crampin, B. Raleigh, and D. Hadley are gratefully acknowledged. This research was supported by the U.S. Geological Survey under Contract 14-08-0001-18321.

References

Backus, G. E. (1965). Possible forms of seismic anisotropy of the uppermost mantle under oceans, *J. Geophys. Res.* **70,** 3429–3439.

Bamford, D. (1976). MOZAIC time-term analysis, *Geophys. J.* **44,** 433–446.

Bamford, D., M. Jentsch, and C. Prodehl (1979). P_n anisotropy studies in northern Britain and the eastern and western United States, *Geophys. J.* **57,** 397–429.

Bird, P. (1980). Fault slip rates, microplate velocities, and mantle flow in southern California, *EOS, Trans. Am. Geophys. Union* **61,** 1125–1126.

Christensen, N. I. and R. S. Crosson (1968). Seismic anisotropy in the upper mantle, *Tectonophysics* **6,** 93–107.

Christensen, N. I. and M. H. Salisbury (1979). Seismic anisotropy in the oceanic upper mantle: evidence from the Bay of Islands ophiolite complex, *J. Geophys. Res.* **84,** 4601–4610.

Claerbout, J. F. (1976). *Fundamentals of Geophysical Data Processing,* McGraw Hill, New York, 274 pp.

Corbett, E. J. and C. E. Johnson (1981). The Santa Barbara, California earthquake of August 13, 1978 (submitted for publication).

Crampin, S. and D. Bamford (1977). Inversion of *P*-wave velocity anisotropy, *Geophys. J.* **49,** 123–132.

Crosson, R. S. (1972). Symmetry of upper mantle anisotropy, *Earth Planet Sci. Letters* **15,** 423–429.

Crosson, R. S. and N. I. Christensen (1969). Transverse isotropy of the upper mantle in the vicinity of Pacific fracture zones, *Bull. Seism. Soc. Am.* **59,** 59–72.

Fuchs, K. (1977). Seismic anisotropy of the subcrustal lithosphere as evidence for dynamical processes in the upper mantle, *Geophys. J.* **49,** 167–179.

Hadley, D. M. (1978). Geophysical investigations of the structure and tectonics of southern California, *Ph.D. Thesis,* California Institute of Technology, Pasadena, California.

Hadley, D. and H. Kanamori (1977). Seismic structure of the Transverse Ranges, California, *Bull. Seism. Soc. Am.* **88,** 1469–1478.

Herrin, E. (1969). Regional variations of *P*-wave velocity in the upper mantle beneath North America, in *The Earth's Crust and Upper Mantle,* P. J. Hart, Editor, *Am. Geophys. Union Monogr.* **13,** 242–246.

Herrin E. and J. Taggart (1962). Regional variations in P_n velocity and their effects in the location of epicenters, *Bull. Seism. Soc. Am.* **52,** 1937–1946.

Hirn, A. (1977). Anisotropy in the continental upper mantle and possible evidence from explosion seismology, *Geophys. J.* **49,** 49–58.

Hutton, K. L., C. R. Allen, A. C. Blanchard, S. A. Fisher, P. T. German, D. D. Given, C. E. Johnson, V. D. Lamanuzzi, B. A. Reed, K. J. Richter, and J. H. Whitcomb (1979). Southern California Array for Research on local earthquakes and teleseisms (SCARLET), Caltech-USGS Monthly Preliminary Epicenters, Seismological Laboratory, California Institute of Technology, Pasadena, California.

Kanamori, H. and D. Hadley (1975). Crustal structure and temporal velocity changes in southern California, *Pageoph* **113,** 257–280.

Kind, R. (1972). Residuals and velocities of P_n-waves recorded on the San Andreas seismograph network, *Bull. Seism. Soc. Am.* **62,** 85–100.

Lachenbruch, A. and J. H. Sass (1980). Heat flow and energetics of the San Andreas fault zone, *J. Geophys. Res.* **85,** 6185–6222.

Marshall, P. D., D. L. Springer, and H. C. Rodean (1979). Magnitude corrections for attenuation in the upper mantle, *Geophys. J.* **57,** 609–638.

Minster, J. B. and T. H. Jordan (1978). Present-day plate motions, *J. Geophys. Res.* **83,** 5331–5354.

Pakiser, L. C. and Steinhart (1964). Explosion seismology in the western hemisphere, *Research in Geophysics,* vol. 2, Solid Earth and Interface Phenomena, Massachusetts Institute of Technology Press, Cambridge, Massachusetts, 123–147.

Parker, R. L. and M. K. McNutt (1980). Statistics for the one-norm misfit measure, *J. Geophys. Res.* **85,** 4429–4430.

Peselnick, L., A. Nicolas, and P. R. Stevenson (1974). Velocity anisotropy in mantle peridotite from the Ivrea zone: application to upper mantle anisotropy, *J. Geophys. Res.* **79,** 1175–1182.

Raitt, R. W., G. G. Shor, T. J. G. Francis, and G. B. Morris (1969). Anisotropy of the Pacific upper mantle, *J. Geophys. Res.* **74,** 3095–3109.

Raleigh, C. B. (1968). Mechanisms of plastic deformation of olivine, *J. Geophys. Res.* **73,** 5391–5406.

Savage, J. C., W. H. Prescott, M. Lisowski, and N. E. King (1981). Strain on the San Andreas fault near Palmdale, California: rapid, aseismic change, *Science* **211,** 56–58.

Snyder, W. S., W. R. Dickinson, and M. L. Silverman (1976). Tectonic implications of space-time patterns of Cenozoic magmatism in the western United States, *Earth Planet Sci. Letters* **32,** 91–106.

Solomon, S. C. and M. N. Toksöz (1970). Lateral variation of attenuation of *P* and *S*-waves beneath the United States, *Bull. Seism. Soc. Am.* **60,** 819–838.

SEISMOLOGICAL LABORATORY
CALIFORNIA INSTITUTE OF TECHNOLOGY
PASADENA, CALIFORNIA 91125
CONTRIBUTION NO. 3574

Manuscript received February 27, 1981